Key Laboratory of Drug Targeting, West China School of Pharmacy, Sichuan University. Chengdu, P.R. China

# Physicochemical characteristics and oral bioavailability of andrographolide complexed with hydroxypropyl-β-cyclodextrin

KE REN, ZHIRONG ZHANG, YANZHEN LI, JIE LIU, DONG ZHAO, YI ZHAO, TAO GONG

*Received February 20, 2009, accepted March 12, 2009*

*Dr. Tao Gong, Key Laboratory of Drug Targeting, Ministry of Education, West China School of Pharmacy, Sichuan University. No. 17, Block 3, Southern Renmin Road, Chengdu 610041, P.R. China*
*gongtaoy@126.com*

*Pharmazie 64: 515–520 (2009)* *doi: 10.1691/ph.2009.9062*

A significant increase in solubility of andrographolide (AND), a slightly water soluble anti-inflammatory and antimicrobial drug, was achieved by inclusion with hydroxypropyl-β-cyclodextrin (HP-β-CD). The inclusion complex was prepared by solvent evaporation and characterized by the phase solubility method, X-ray diffractometry and differential scanning calorimetry. The solubility of AND increased linearly as a function of HP-β-CD concentration, resulting in $A_L$-type phase solubility diagram. Molecular modeling calculations were used to foresee the possible orientations of AND inside the HP-β-CD cavity. The *in vitro* dissolution profile showed a significant increase in dissolving rate and percent of the inclusion complex compared with uncomplexed drug. *In vivo* pharmacokinetic study showed that $AUC_{0-\infty}$ was 1.6-fold higher than that of AND suspension after oral administration. These results suggest that HP-β-CD inclusion system might be a promising formulation for the oral delivery of AND.

## 1. Introduction

*Andrographis paniculata* (Burm. F.) Nees is one of the most important medicinal herbs in China. This herb has been used traditionally for several applications such as anticancer (Kumar et al. 2004), anti-inflammory (Sheeja et al. 2006), anti-angiogenic (Sheeja et al. 2007) and against HIV (Calabrese et al. 2000). The main medicinal component of this herb is andrographolide (AND), the structure of which is shown in Fig. 1. It has been extensively used in the management of gastroenteritis, bacillary dysentery and acute tonsillitis.

Tablets and capsules are commonly used dosage forms for AND. Unfortunately, due to AND's poor water-solubility (about 74 $\mu g \cdot mL^{-1}$ in water at 25 °C), the oral bioavailability of AND is very low (Ou et al. 2000). Therefore, to increasing its oral bioavailability by enhancing its water solubility using a pharmaceutical carrier seems necessary and urgent.

Cyclodextrins (CDs) are cyclic oligosaccharides made up of six (α-CD), seven (β-CD), or eight (γ-CD) D-glucopyranose units which can trap lipophilic drug as guests in a cage-like meshwork, thereby enhancing solubility and dissolution rate (Palmieri et al. 1997; Castillo et al. 1999). Among the CDs, hydroxypropyl-β-cyclodextrin (HP-β-CD), which has higher water solubility, lower renal toxicity and haemolytic activity (Loftsson and Brewster 1996; Agu et al. 2000), has been approved by the FDA for the use of many drugs including itraconazole, cisapride and mitomycin (Loftsson and Duchêne, 2007).

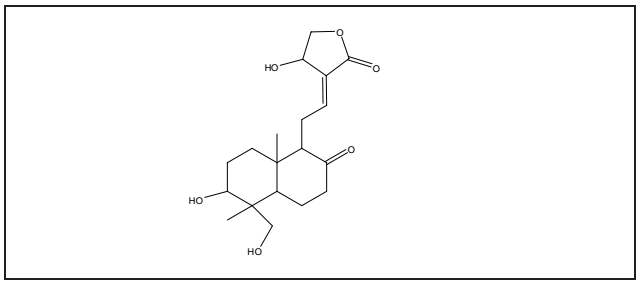


Fig. 1: Chemical structure of AND

The goal of this study was to enhance the water solubility of AND by HP-β-CD, research on the physicochemical characteristics of the inclusion complex and evaluate its oral bioavailability. In the present work, we achieved complexation of AND with HP-β-CD by a solvent evaporation method and characterized it by X-ray diffractometry (XRD), differential scanning calorimetry (DSC) and phase solubility method. Hyperchem 7.5 was used to elucidate the structure of the inclusion. The dissolution rate and oral bioavailability were compared among complexion, physical mixture and AND powder.

## 2. Investigations, results and discussion

### *2.1. Characterization of the inclusion complexes*

Some evidence of inclusion complex (IC) was obtained from thermal analysis. When guest molecules were embedded in HP-β-CD cavities, their melting, boiling or sublimation point generally could shift to a different temperature or disappear within the temperature range where HP-β-CD was decomposed. The thermograms of AND and HP-β-CD corresponding binary systems are shown in Fig. 2.

AND showed a characteristic endothermic peak corresponding to its melting point (235 °C). Meanwhile, it had an exothermic peak at about 280 °C which might be

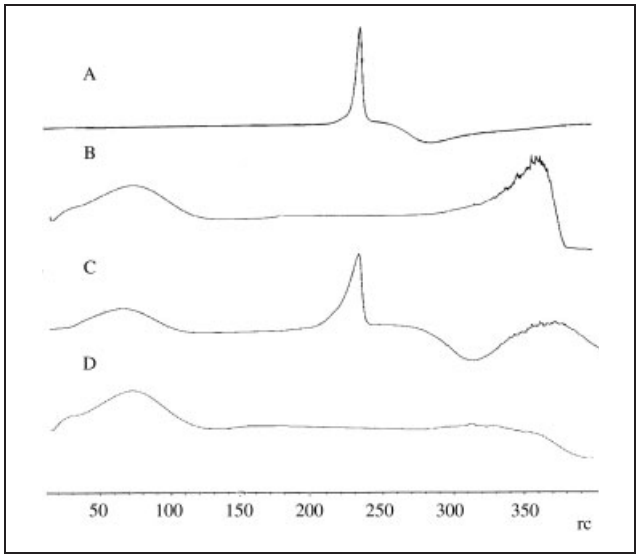


Fig. 2: DSC thermograms of (A) AND, (B) HP-β-CD, (C) PM and (D) IC

caused by the decomposing of the drug (Fig. 2A). The thermogram of HP-β-CD showed a very broad endothermic effect, which attained a maximum around 75 °C, due to the release of bound water in the cavity (generally HP-β-CD has about 3% water) (Fig. 2B) (Miro et al. 2004). Besides, the base shift around 350 °C may result from a decomposition process. The thermogram of the physical mixture (PM) of AND with HP-β-CD (Fig. 2C), was the sum of those of the components analyzed separately. This thermogram indicated by the absence of interaction between AND and HP-β-CD, that in a PM system an inclusion complex could not be obtained by simple blending the drug and HP-β-CD. As can be seen in Fig. 2D, the AND endothermic peak disappeared completely for the inclusion complex (IC) since the AND molecule was contained within the cavity of the HP-β-CD ring molecule (Zi et al. 2008). This demonstrated that an inclusion complex could be obtained by the coevaporation method.

Further evidence for the formation of AND/HP-β-CD complexes was obtained by XRD patterns as demonstrated in Fig. 3. In the X-ray diffractogram of AND powder (Fig. 3A), crystalline peaks at diffraction angles were present suggesting that the drug was present as a crystalline material (Choi et al. 2003). The absence of any peak in the HP-β-CD diffractogram revealed the amorphous nature of this compound as shown in Fig. 3B. The diffraction profile of PM was found to be the simple superimposition of each component, with the crystalline peaks of AND emerging on the diffuse background of the amorphous carrier and having a lower intensity (Fig. 3C). This was due to a reduction in particle size during the preparation of the physical mixture and to the dilution of AND in the physical mixture. The complex system did not exhibit peaks corresponding to AND and displayed a completely diffuse diffraction pattern, indicating the entirely amorphous nature of AND in the complex (Fig. 3D). X-ray powder diffraction patterns confirmed the results of DSC analysis, showing that an inclusion complex between AND and HP-β-CD was formed by the coevaporation method.

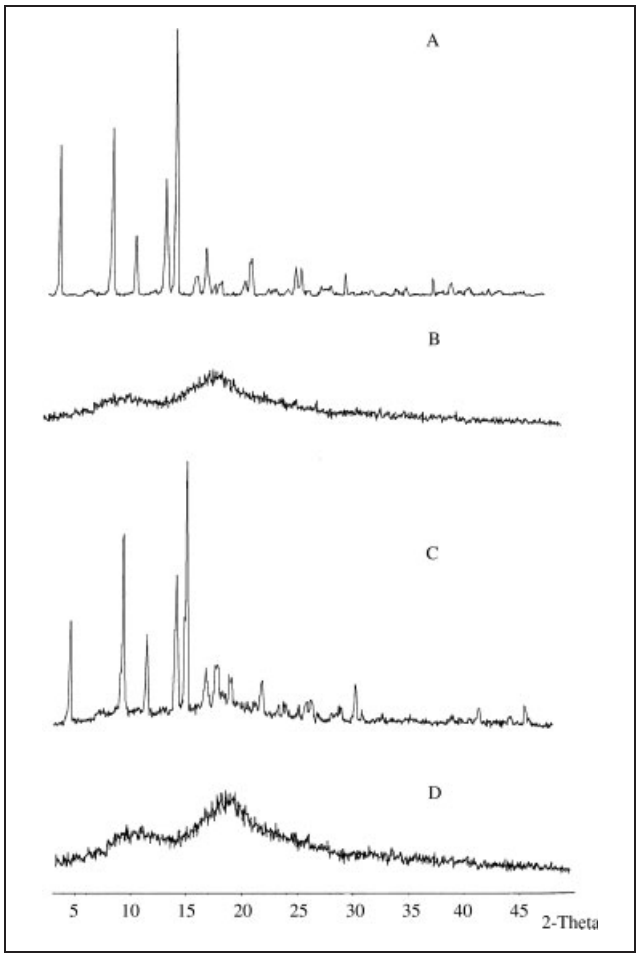


Fig. 3: X-ray diffractograms of (A) AND, (B) HP-β-CD, (C) PM and (D) IC

### *2.2. Phase solubility studies*

The solubility method is useful for studying inclusion compounds of poorly soluble drugs with CDs in water because it gives not only the solubilizing ability of CDs but also the stability constant ($K_C$) of the complexes by analyzing the solubility curves. The phase solubility diagrams of AND/HP-β-CD obtained in water at different temperatures are shown in Fig. 4. The diagram showed that the aqueous solubility of the drug increased linearly as a function of HP-β-CD concentration, over the entire concentration range studied. All the solubility curves with correlation coefficient squared values ($r^2$) $> 0.990$ ($r^2 = 0.995$) were regarded as a straight line ($A_L$ type) (Higuchi and Connors 1965). The intrinsic solubility ($S_0$) of AND in water at 25 °C was determined to be 212 $\mu Mol \cdot L^{-1}$ (74 $\mu g \cdot mL^{-1}$). Subsequently, the stoichiometry 1 : 1 apparent stability constant of the complex was calculated from the slope of the straight line of the phase-solubility diagram according to Eq. 1:

$$Kc = slope/S_0(1 - slope) \quad (1)$$

Here $S_0$ is the solubility of the pure drug at the same temperature in water. From this equation we could get the Kc under 25, 35 and 45 °C. According to Gibbs and Van't Hoff equations:

$$\lg Kc = \frac{-\Delta H}{2.303\,RT} + \frac{\Delta S}{2.303\,R} \quad (2)$$

a plot of lg Kc versus 1/T produces:

$$\lg Kc = 709.97\ \frac{1}{T} + 0.811 \quad (3)$$

Slope $= -\Delta H/2.303\,R$, intercept $= \Delta S/2.303R$, $\Delta G = \Delta H - T\Delta S$.

**Table 1: Thermodynamic parameters of AND/HP-β-CD inclusion effects**

| Temperature (°C) | Regression equation | r | Kc ($L \cdot mol^{-1}$) | ΔG ($kJ \cdot mol^{-1}$) | ΔH ($kJ \cdot mol^{-1}$) | ΔS ($J\ k^{-1}.mol^{-1}$) |
|---|---|---|---|---|---|---|
| 25 | $y = 0.2475x - 0.0011$ | 0.9990 | 1551.4 | −18.20 | | |
| 35 | $y = 0.2578\ x - 0.0008$ | 0.9988 | 1321.4 | −18.40 | −13.59 | 15.53 |
| 45 | $y = 0.2638\ x - 0.0001$ | 0.9990 | 1099.2 | −18.51 | | |

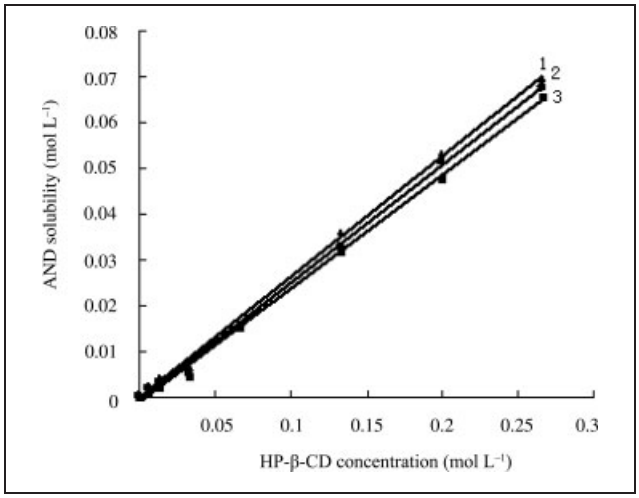


Fig. 4: Phase solubility diagrams of the AND/HP-β-CD at different temperatures: (1) 45 °C, (2) 35 °C and (3) 25 °C

The corresponding complex formation constants (Kc) and the thermodynamic parameters (ΔH, ΔS and ΔG) are shown in Table 1.

According to the thermodynamic parameters, the stability constant (Kc) decreases with increasing temperature which indicates that temperature has a negative impact on the formation of the inclusion. Meanwhile, the results suggest that complex formation for AND is largely driven by enthalpy ($\Delta H = -13.59\ kJ \cdot mol^{-1}$) and slight entropy ($S = 15.53\ J \cdot mol^{-1}\ K^{-1}$) changes, which are attributed to van der Waals interaction and solvent disordering.

### *2.3. Molecular modeling*

According to the consequence of $MM^{+}$ calculations, the structures of A and D (both the two rings of naphthaline group inserted into the HP-β-CD through the wide and narrow rims proved to be inexistent, since the two rings of naphthaline group of AND would be pushed out of the range of HP-β-CD when the energy is minimized

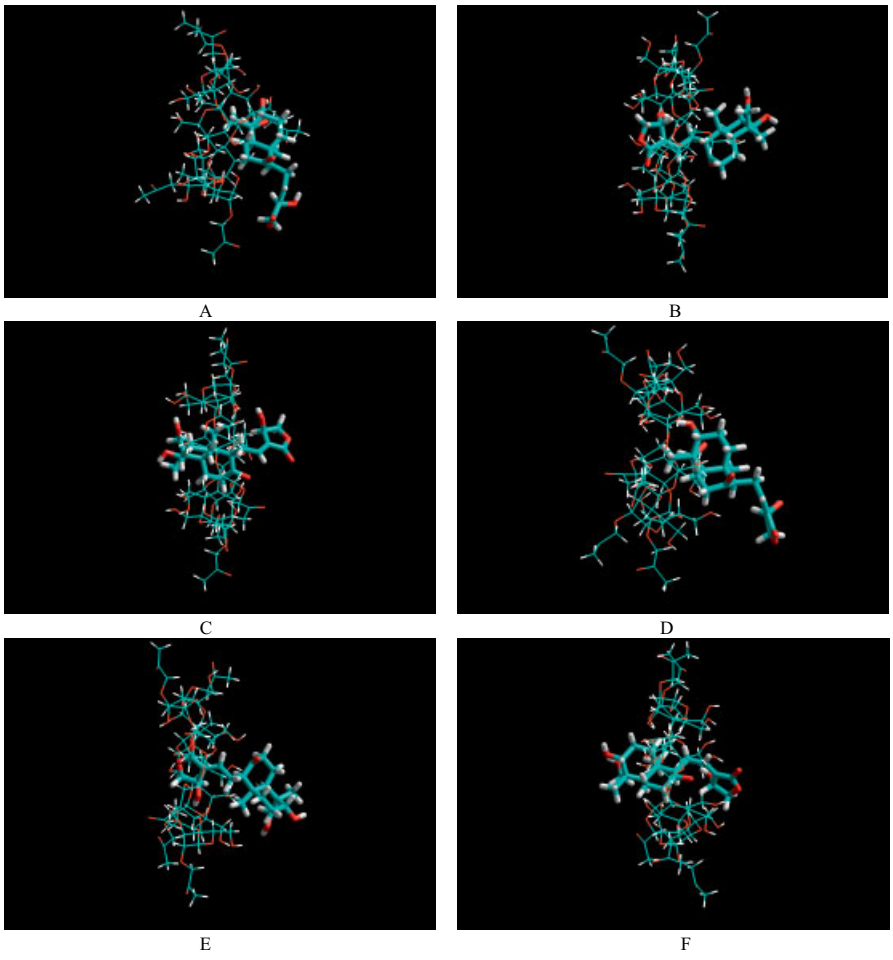


Fig. 5:
Optimized structures of AND/HP-β-CD complexes: (A) naphthaline (two rings) in wide rim, (B) furan in wide rim, (C) naphthaline (partial) in wide rim, (D) naphthaline (two rings) in narrow rim, (E) furan in narrow rim and (F) naphthaline (partial) in narrow rim

**Table 2: Molecular modeling results of interaction energies of AND/HP-β-CD inclusion complexes (1 : 1). (Unit: kcal mol$^{-1}$)**

| Approach included moiety | Wide rim | | | Narrow rim | | |
|---|---|---|---|---|---|---|
| | Naphthaline (two rings) | Furan | Naphthaline (partial) | Naphthaline (two rings) | Furan | Naphthaline (partial) |
| Signal | A | B | C | D | E | F |
| $E_{binding}$ | – | −28.77 | −12.24 | – | −27.02 | −17.63 |
| $E_{bond}$ | – | −0.74 | 0.24 | – | −0.68 | 0.26 |
| $E_{angle}$ | – | 1.24 | 4.01 | – | −0.49 | 4.26 |
| $E_{dihedral}$ | – | 3.23 | 11.08 | – | 3.54 | 7.74 |
| $E_{vdw}$ | – | −31.25 | −29.16 | – | −29.33 | −28.44 |
| $E_{strech\text{-}bond}$ | – | 0.12 | 1.09 | – | 0.15 | 0.87 |
| $E_{electrostatic}$ | – | −1.37 | 0.48 | – | −0.23 | −2.32 |

(Fig. 5A, 5D). The binding energies ($E_{binding}$) with their $E_{bond}$, $E_{angle}$, $E_{dihedral}$, $E_{vdw}$, $E_{strech\text{-}bond}$, $E_{electrostatic}$ for the other four possibilities of 1 : 1 complexation are listed in Table 2. The dominant driving force for complexation is evidently van der Waals contribution. The furan approach (Fig. 5B, 5E) through the wide and narrow rims proved to be the most energetically favorable route towards inclusion of AND into the HP-β-CD cavity leading to complete inclusion of the furan group leaving the naphthaline substituent situated outside of the cavity.

### *2.4. Dissolution studies*

The dissolution profiles are shown in Fig. 6. The dissolution efficiency parameter was evaluated by the mean percentage of dissolved AND at 60 min, according to the regulations of CHP2005. As could be seen from Fig. 6, the HP-β-CD complex exhibited faster dissolution than the corresponding PM and the free AND, being immediately dispersed and completely dissolved within 10 min. The uncomplexed AND dissolved only to the extent of 11.81% after 60 min. The percentage of AND dissolved from the PM and IC was 31.9% and 98.6%, respectively. These facts were consistent with the results of the solubilizing activity of HP-β-CD, suggesting that the enhancing effect of HP-β-CD on the dissolution rate of AND could be explained from the enhanced aqueous solubility of AND after the formation of complexation. In addition, according to literature suggestions (Szejtli et al. 1994), a decrease in crystallinity of the drug might be the other factor in the enhanced dissolution by the complex besides an increase in solubility.

### *2.5. Pharmacokinetics and statistical analysis*

Pharmacokinetic parameters were determined by fitting pharmacokinetic models to the plasma concentration-time profiles for each rat after oral administration. From the results of kinetic analysis, a two-compartment open model with 1 weighting coefficient was considered the most appropriate pharmacokinetic model.

The peak concentrations ($C_{max}$) for the physical mixture and the inclusion complexes were 1.3- and 2.0- fold higher, respectively, than that for the AND powder (shown in Fig. 7). AUC values followed the same trend as the $C_{max}$ values: the AUC after administration of the inclusion complexes were about 1.6 times higher than those after administration of AND suspension. Meanwhile, the absorption phase observed with the inclusion complexes (about 40 min) was shorter than that achieved after administration of AND suspension (about 60 min). The pharmacokinetic parameters are listed in Table 3.

In conclusion, this study demonstrated that AND formed 1 : 1 inclusion complexes with HP-β-CD. Molecular modeling calculations revealed the furan approach (Fig. 8B, 8E) through the wide and narrow rims proved to be the most energetically favorable route towards inclusion of AND into the HP-β-CD cavity. Inclusion complex of the

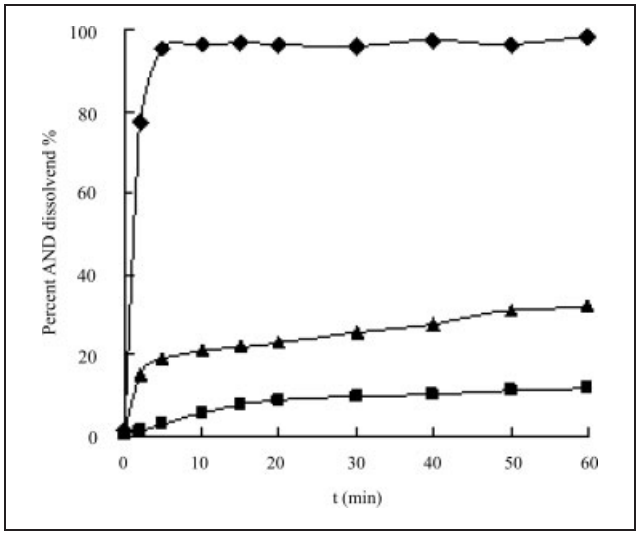


Fig. 6: Dissolution profiles of (■) free AND, (▲) PM and (□) IC

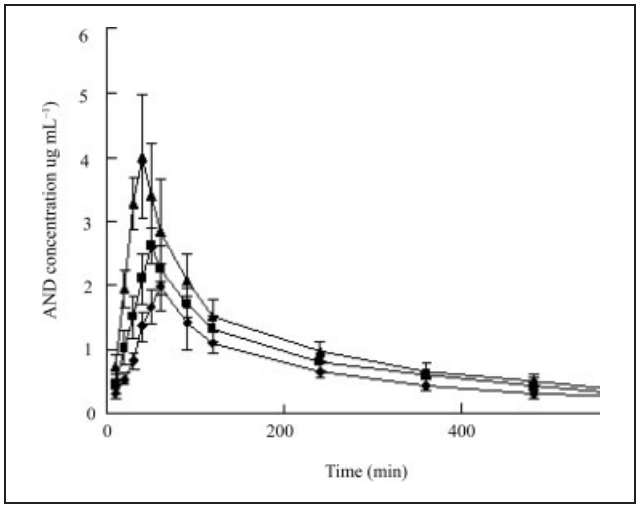


Fig. 7: Mean plasma concentration-time curves of (▲) IC, (■) PM and (◆) AND after oral administration to rats (n = 6)

**Table 3: Pharmacokinetic parameters (mean ± S.D.) obtained after oral administration (25 mg kg$^{-1}$) to rats (n = 6)**

| | | AND | PM | IC |
|---|---|---|---|---|
| $AUC_{0-t}$ | $mg \cdot L^{-1}min^{-1}$ | 426.00 ± 67.81 | 545.74 ± 100.62 | 681.47 ± 113.92 |
| $AUC_{0-\infty}$ | $mg \cdot L^{-1}\ min^{-1}$ | 482.01 ± 88.56 | 623.79 ± 127.94 | 751.29 ± 132.40 |
| $C_{max}$ | $mg \cdot L^{-1}$ | 2.07 ± 0.27 | 2.66 ± 0.27 | 4.10 ± 0.92 |
| $T_{max}$ | min | 61.67 ± 14.72 | 50.00 ± 8.94 | 41.67 ± 11.69 |

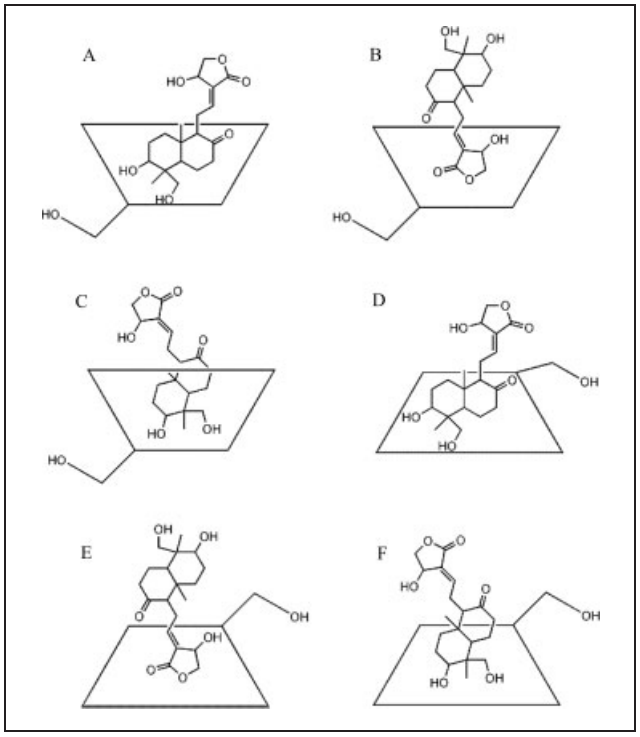


Fig. 8: Schematic representation of the starting orientations of AND/HP-β-CD (1 : 1 stoichiometry) used in the molecular modeling calculations. (A) naphthaline (two rings) in wide rim, (B) furan in wide rim, (C) naphthaline (partial) in wide rim, (D) naphthaline (two rings) in narrow rim, (E) furan in narrow rim and (F) naphthaline (partial) in narrow rim

drug was remarkably less crystalline and, therefore, more soluble than the AND itself in aqueous media. In addition, the dissolution degree and rate were greatly enhanced by inclusion process. *In vivo* studies showed that $C_{max}$ and AUC were significantly different ($p < 0.05$) between inclusion complex and AND powder. Meanwhile, a lower $T_{max}$ was observed for the inclusion complex.

The use of this multicomponent system provided a new way to enhance the oral bioavailability of AND with higher absorption rate, which was mainly due to the increase in the drug's solubility and dissolution rates.

## 3. Experimental

### *3.1. Materials*

AND (99.54%, $C_{20}H_{30}O_5$, MW = 350.44) was purchased from Sichuan Wenlong Medical Development Co.Ltd (Chengdu, China), and AND standard was purchased from the National Institute for the Control of Biological and Pharmaceutical Drugs (PR China). HP-β-CD (average MW = 1429), degree of substitution (DS) = 7, was purchased from Xi'an Deli Chemicals Corporation. Carbamazepine was obtained from the National Institute for the Control of Biological and Pharmaceutical Drugs (PR China). Methanol (HPLC grade) was from Yucheng Chemical Plant of Shandong Yuwang Industrial Ltd. All other reagents and solvents used in this experiment were of the highest purity commercially available. Water was prepared in an ultra pure water system.

### *3.2. Animals*

Healthy Sprague-Dawley rats (six males and six females) (200 ± 20 g) were obtained from Laboratory Animal Center of Sichuan University, Sichuan (PR China). Prior to the experiments, the rats were housed in a temperature and humidity controlled room (25 ± 1 °C, 55% air humidity) with free access to water and standard rat chow. The rats were acclimated for at least 5 days and fasted overnight but supplied with water before the experiments. All experiments were approved by the Institutional Animal Care and Use Committee of Sichuan University.

### *3.3. Preparation of the inclusion complexes and physical mixture of AND and HP-β-CD*

Inclusion complex: The AND/HP-β-CD inclusion complexes were prepared by coevaporation with the weights taken for 1.05 g of AND and 4.28 g of HP-β-CD (i.e. molar ratio of 1 : 1). The required stoichiometric amount of AND and HP-β-CD were dissolved in the minimum amount of 50% ethanol to obtain a solution, and agitated for 5 h at 50 °C. Then, the suspension was filtered through a 0.45 μm Millipore filter. The filtrate was evaporated under vacuum at 40 °C and 100 rpm in a rotary evaporator (Büchi Rotavapor R-114, Switzerland) until dryness.

Physical mixture: A physical mixture of AND and HP-β-CD in the same weight ratio as the coevaporated complex was prepared. PM was previously sieved individual components through a 315 μm mesh in a mortar and pestle for 3 min.

### *3.4. Characterization of the inclusion complexes*

#### *3.4.1. Differential scanning calorimetry*

Approximately 10 mg of AND, HP-β-CD, PM and IC were subjected to DSC analysis, using a DSC-200PC (Schneider, German). Alumina was used as a reference material and the scanning rate was 10.00 °C · min$^{-1}$, with the scanning temperature range of 25 and 400 °C.

#### *3.4.2. Powder X-ray diffractometry*

Powder X-ray diffraction patterns were obtained from a Philips X'Pert, model PW3040/00 diffractometer. Samples were irradiated with monochromatized Cu/Kα radiation and analyzed between a 2θ range of 5–70° (where theta is the scattering angle) with a step size of 0.05° (2θ).

### *3.5. Determination of AND*

Concentrations of AND were determined by high-pressure liquid chromatography (HPLC). The HPLC system consisted of a Waters 2690 separation module and a 996 Photodiode Array (PDA) detector; and data were collected and processed using Millennium software version 3.2 (all equipment from Waters, Milford, MA, USA). Chromatographic separations were carried out on a Hypersil ODS2 $C_{18}$ column (5 μm, 150 mm × 6.0 mm, physical chemistry institute of Chinese Academy, China) equipped with a Shimadzu Shim-pack G guard column ($C_{18}$, 10 mm × 4 mm, 5 μm) (Chiyoda-Ku, Tokyo, Japan). The mobile phase consisted of water and methanol (50 : 50, v/v), freshly prepared daily and filtered through a 0.22 μm membrane filter and degassed via an online degasser. The injection volume was 25 μL each and eluted at a flow rate of 1.0 mL · min$^{-1}$ at 35 °C. The eluents were monitored at 226 nm.

### *3.6. Phase solubility studies*

Solubility measurements were carried out according to a modification of the method of Higuchi and Connors (1965). Excess amounts of AND were added to 10 mL of aqueous solutions containing various concentration of HP-β-CD (0–$266.13 \times 10^{-3}$ mol · L$^{-1}$). The suspensions were shaken for 3 days on a shaker (100 r · min$^{-1}$) to equilibrate at 25 ± 0.1, 35 ± 0.1, 45 ± 0.1 °C respectively. After equilibration, the suspensions were filtered through 0.45 μm Millipore membrane filters. The first 15% of the filtrate were discarded to avoid any potential loss of the drug, because of absorption by the filter and the subsequent filtrate was collected. All procedures were conducted at the test temperature to avoid any precipitation of the drug. The filtrate was appropriately diluted by water and the concentration of the AND in the filtrate was determined by HPLC. Earlier experiments showed that the presence of HP-β-CD did not interfere with the assay at the concentration employed.

### *3.7. Molecular modeling*

Calculations by the MM$^+$ force field using HyperChem7.5 software (Hypercube, Canada) were performed in order to obtain the 3D geometry of AND and HP-β-CD molecules, alone and in the complex, with a rms less

than 0.01 kcal $mol^{-1}$. The energetic of the interaction were simulated in vacuum, where water molecules were ignored to save computational time especially for large molecule (Tong et al. 1991; Omari et al. 2006). The previously optimized structures of AND and HP-β-CD molecules were allowed to approach each other along the symmetric axis (the x-axis) passing through the center of the HP-β-CD cavity. Fig. 8 shows six starting orientations of the most possible stable AND/HP-β-CD (1 : 1 stoichiometry).

In the $MM^+$ calculations, we considered the relative thermodynamic relationship as the proportional stability of the complex formation. Interaction energies were calculated for the drug approaching from its certain group through the wide and narrow rims of HP-β-CD cavity to access the most probable optimal configurations for the complex formed. The binding energy $E_{binding} = E_{complex} - (E_{andrographolide} + E_{HP\text{-}\beta\text{-}CD})$ was plotted for each longitudinal approach to indicate the energy minima. Accordingly, $E_{bond}$, $E_{angle}$, $E_{dihedral}$, $E_{vdw}$, $E_{strech\text{-}bond}$, $E_{electrostatic}$ are calculated from the method: energy of the inclusion complex minus sum energy of each part in their respective equilibrium geometry (Jesus et al. 2006).

### *3.8. Dissolution studies*

The *in vitro* dissolution studies were conducted according to the CP2005 in the deionized water at $37 \pm 0.5\,^{\circ}C$ by the paddle method at a rotation speed of $100 \pm 2$ rpm using a six-vessel dissolution apparatus (Beckman, DU-65, USA). Powdered samples containing 50 mg of AND or its equivalent in IC or PM with HP-β-CD were added to the dissolution medium (100 mL). At predetermined time intervals (2, 5, 10, 15, 20, 30, 40, 50 and 60 min), aliquots (0.5 mL) were withdrawn for HPLC determination of AND concentration following filtration (0.45 μm) and replaced by an equal volume of the same dissolution medium kept at $37 \pm 0.5\,^{\circ}C$. Samples should be withdrawn from a zone roughly midway between the surface of dissolution medium and the top of the rotating blade. Each experiment was carried out in triplicate.

### *3.9. Animal experiment*

#### *3.9.1. HPLC Method validation*

The retention time of AND and internal standard (IS) carbamazepine were 6.3 and 9.4 min, respectively. Control plasma samples taken prior to drug treatment showed that there are no peaks that interfere with the AND or IS signals. The mean regression equation for AND in plasma was $y = 0.023x + 0.0177$ ($r = 0.9990$, $n = 6$), where y is the peak area ratio of each compound to IS and x is the concentration. These equations show that there is significant linearity over the concentration range of 0.1–10 $\mu g \cdot mL^{-1}$. Variations for both precision and accuracy of the inter- and intra-day results never exceeded 15%. The mean absolute recovery of AND in plasma was over 96%.

#### *3.9.2. Drug administration and plasma sample collection*

Oral administration with AND and its equivalent in IC or PM with HP-β-CD at a dose of 25 $mg \cdot kg^{-1}$ was performed after suspending the materials in distilled water just prior to use. Serial blood samples (0.3 mL) were obtained from the tail into heparinized tubes 10, 20, 30, 40, 50, 60, 90, 120, 240, 360, 480, 600 and 720 min after drug administration. Plasma samples were obtained following centrifugation at $4000 \times g$ for 4 min.

#### *3.9.3. Sample Preparation*

Plasma (100 μL) was mixed with 100 μL of the IS solution and 40 μL 10% trichloracetic acid and vortexed for 2 min, the mixture was centrifuged at $10000 \times g$ for 20 min. A 20 μL aliquot of the supernatant was injected into the HPLC system.

#### *3.9.4. Pharmacokinetics data analysis*

The data were analyzed using non-linear regression analysis by the computer program DAS 2.0 (Drug and Statistics, Anhui, China).

Acknowledgements: The present work was funded by the 973 Program of Chinese government (No. 2009C930300) and supported by the National Science Foundation of PR China (No.30430770).

**References**

Agu RU, Jorissen M, Willems T, Mooter GV, Kinget R, Verbeke N, Augustijns P (2000) Safety assessment of selected cyclodextrins-effect on ciliary activity using a human cell suspension culture model exhibiting in vitro ciliogenesis. Int J Pharm 193: 219–226.

Calabrese C, Berman SH, Babish JG, Ma X, Shinto L, Dorr M (2000) A phase I trail of andrographolide in HIV positive patients and normal volunteers. Phytother Res 14: 333–338.

Castillo JA, Canales JP, Garcia JJ, Lastres JL, Bolas F, Torrado JJ (1999) Preparation and characterization of albendazole-β-cyclodextrin complexes. Drug Dev Ind Pharm 25: 1241–1248.

Choi HG, Kim DD, Jun HW, Yoo BK, Yong CS (2003) Improvement of dissolution and bioavailability of nitrendipine by inclusion in hydroxypropyl-β-cyclodextrin. Drug Dev Ind Pharm 29: 1085–1094.

Higuchi T, Connors KA (1965) Phase solubility techniques. Adv Anal Chem Instrum 4: 117–122.

Jesus MB, Pinto LM, Fraceto LF, Takahata Y, Lino ACS, Jaime C, Paula E (2006) Theoretical and experimental study of a praziquantel and β-cyclodextrin inclusion complex using molecular mechanic calculations and $^1$H-nuclear magnetic resonance. J Pharm Biomed Anal 41: 1428–1432.

Kumar RA, Sridevi K, Kumar NV, Nanduri S, Rajagopal S (2004) Anticancer and immunostimulatory compounds from Andrographis paniculata. J Ethnopharmacol 92: 291–295.

Loftsson T, Duchêne D (2007) Cyclodextrins and their pharmaceutical applications. Int J Pharm 329: 1–11.

Loftsson T, Brewster ME (1996) Pharmaceutical applications of cyclodextrins. I. Drug solubilization and stabilization. J Pharm Sci 85: 1017–1025.

Miro A, Quaglia F, Sorrentino U, La Rotonda MI, D'Emmanuele Di Villa Bianca R, Sorrentino R (2004) Improvement of gliquidone hypoglycaemic effect in rats by cyclodextrin formulations. Eur J Pharm Sci 23: 57–64.

Omari MM, Zughul MB, Davies JE, Badwan AA (2006) Sildenafil/cyclodextrin complexation: Stability constants, thermodynamics, and guest-host interactions probed by $^1$H NMR and molecular modeling studies. J Pharm Biomed Anal 41: 857–865.

Ou WP, Ye SM, Mi HQ, Hong X (2000) Comparison of bioavailability between chuanxinlian capsule and chuanxinlian Pill. Chin J Integr Med 1: 8–10.

Palmieri, GF, Angeli DG, Giovannucci G, Martelli S (1997) Inclusion of methoxybutropate in β- and hydroxypropyl-β-cyclodextrins: comparison of preparation methods. Drug Dev Ind Pharm 23: 27–37.

Sheeja K, Guruvayoorappan C, Kuttan G (2007) Antiangiogenic activity of andrographis paniculata extract and andrographolide. Int Immunopharmacol 7: 211–221.

Sheeja K, Shihab PK, Kuttan G (2006) Antioxidant and antiinflammatory activities of the plant Andrographis paniculata Nees. Immunopharmacol Immunotoxicol 28: 129–140.

Szejtli J (1994) Medicinal applications of cyclodextrins. Med Res Rev 14: 353–386.

Tong WQ, Lach JL, Chin TF, Guillory JK (1991) Structural effects on the binding of amine drugs with the diphenylmethyl functionality to cyclodextrins. II. Amolecular modeling study. Pharm Res 8: 1307–1312.

Zi P, Yang XH, Kuang HF, Yang YS, Yu LL (2008) Effect of HP-β-CD on solubility and transdermal delivery of capsaicin through rat skin. Int J Pharm 358: 151–158.